Correlation between Fermi surface reconstruction and superconductivity in pressurized $FeTe_{0.55}Se_{0.45}$

Gongchang Lin,[1,3,*] Jing Guo,[1,4,*] Yanglin Zhu,[2] Shu Cai,[1] Yazhou Zhou,[1] Cheng Huang,[1,3] Chongli Yang,[1] Sijin Long,[1,3] Qi Wu,[1] Zhiqiang Mao,[2] Tao Xiang,[1,3] and Liling Sun[1,3,4,†]

[1]*Institute of Physics, National Laboratory for Condensed Matter Physics, Chinese Academy of Sciences, Beijing 100190, China*
[2]*Department of Physics, Pennsylvania State University, University Park, Pennsylvania 16802, USA*
[3]*Department of Physics, University of Chinese Academy of Sciences, Beijing 100190, China*
[4]*Songshan Lake Materials Laboratory, Dongguan, Guangdong 523808, China*

(Received 1 April 2020; revised manuscript received 13 June 2020; accepted 17 June 2020; published 30 June 2020)

Here we report the results of the high-pressure Hall coefficient (R_H) measurements, combined with the high-pressure resistance measurements, at different temperatures on the putative topological superconductor $FeTe_{0.55}Se_{0.45}$. We find the intimate correlation of sign change of R_H, a fingerprint to manifest the reconstruction of Fermi surface, with structural phase transition and superconductivity. Below the critical pressure (P_c) of 2.7 GPa, our data reveal that the hole-electron carriers are thermally balanced ($R_H = 0$) at a critical temperature (T^*), where R_H changes its sign from positive to negative, and concurrently a tetragonal-orthorhombic phase transition takes place. Within the pressure range from ambient pressure to P_c, T^* is continuously suppressed by pressure, while T_c increases monotonically. At about P_c, T^* is undetectable and T_c reaches a maximum value. Moreover, a pressure-induced sign change of R_H is found at $\sim P_c$ where the orthorhombic-monoclinic phase transition occurs. With further compression, T_c decreases and disappears at $\sim$ 12 GPa. The correlation among the electron-hole balance, crystal structure, and superconductivity found in the pressurized $FeTe_{0.55}Se_{0.45}$ implies that its nontrivial superconductivity is closely associated with its exotic normal state resulting from the interplay between the reconstruction of the Fermi surface and the change of the structural lattice.

DOI: 10.1103/PhysRevB.101.214525

The discovery of Fe-based superconductors provides a platform not only for understanding the microscopic mechanism of high-temperature superconductivity beyond the copper oxide superconductors [1,2], but also for finding phenomena from correlated electron systems. Among Fe-based superconductors, iron selenide (FeSe) is distinct; it has the simplest crystal structure [3] and shows the sensitive effect of pressure on the superconducting transition temperature (T_c) [4,5]. The isovalent substitution Se with Te in FeSe superconductors can increase T_c from 8 K to about 15 K [6–8], and more attractively, an unusual interplay between the resonance and the incommensurate magnetism has been found only in the crystals with an average composition near $FeTe_{0.5}Se_{0.5}$ [7,9,10]. Intriguingly, recent high-resolution angle-resolved photoelectron spectroscopy (ARPES) and scanning tunneling spectroscopy experiments find the evidence for Dirac-cone type spin-helical surface states [11] and Majorana bound states in a $FeTe_{0.55}Se_{0.45}$ superconductor [12], which is a signature of topological superconductivity. These findings have renewed research interest in this material. One particularly interesting direction is to explore the variation of its electronic state with lattice structure. Results from such work are expected to reveal insights into the nature of the topological superconductivity of this material.

In general, the unconventional superconductivity of a given material is dictated by multiple degrees of freedom of charge, spin, orbital, and lattice. These degrees of freedom as well as the interactions among them can be manipulated by control parameters such as pressure, magnetic field, and chemical doping [13–18]. Pressure tuning is a clean way to provide significant information on coevolution among superconductivity, electronic state, and crystal structure without changing the chemistry, and to result in a deeper understanding of the underlying physics of the exotic state emerging from ambient-pressure materials. In this study, we performed *in situ* high pressure transport measurements on the high quality single crystals of $FeTe_{0.55}Se_{0.45}$, with the attempt to find such kind of coevolution information.

The single crystals with nominal composition of $FeTe_{0.55}Se_{0.45}$ were grown using a flux method [19]. The values of the midpoint T_cs of the samples from the two batches were determined to be 13.5 and 13.7 K, respectively (see the Supplemental Material [20]). High pressure was generated by a diamond anvil cell made of BeCu alloy with two opposing anvils. A four-probe method was applied for our resistance measurements. Diamond anvils with 300 and 400 μm culets (flat area of the diamond anvil) were used for several independent measurements. In the experiments, we employed platinum foil as electrodes, rhenium plate as

*These authors contributed equally to this work.
†To whom correspondence may be addressed: llsun@iphy.ac.cn

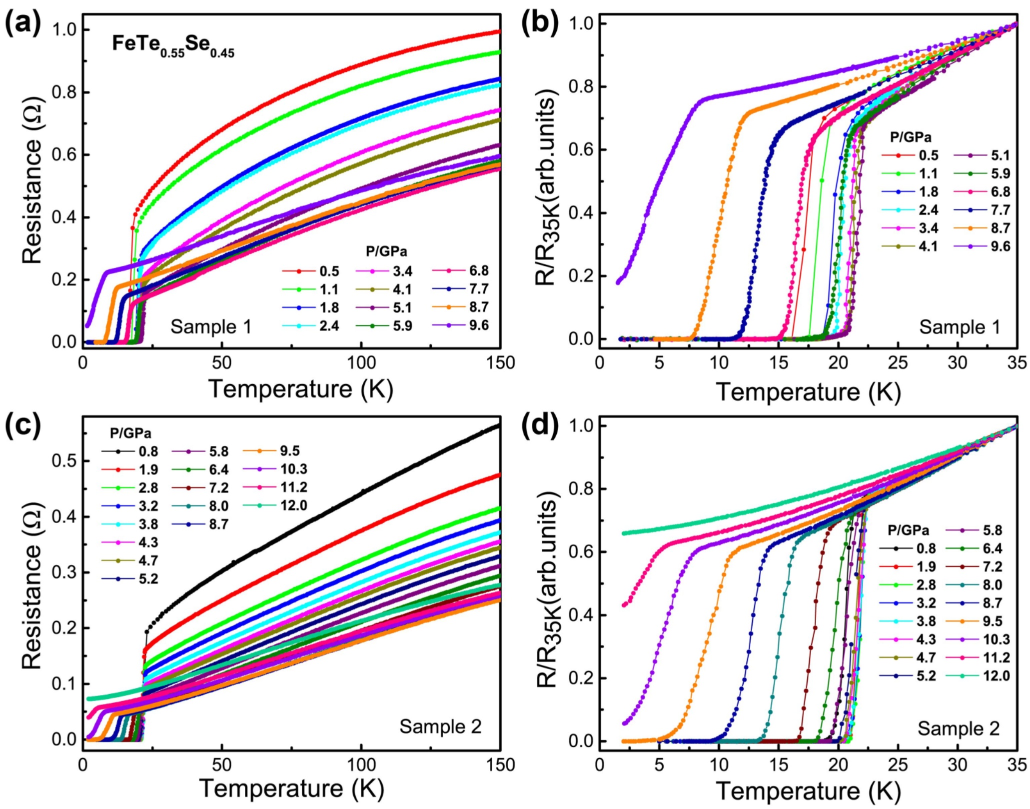

FIG. 1. The superconducting behavior of $FeTe_{0.55}Se_{0.45}$ at high pressures. (a) Temperature dependence of the resistance in the pressure range of 0.5–9.6 GPa for sample 1. (b) Enlarged views of the resistance in the lower temperature for sample 1. (c) Resistance as a function of temperature for pressures ranging from 0.8 GPa to 12 GPa for sample 2. (d) Resistance versus temperature near the superconducting transition of sample 2.

gasket, cubic boron nitride as insulating material and NaCl as pressure medium. A high-pressure Hall coefficient was measured through Van der Pauw method under magnetic field generated from a superconducting coil (see the Supplemental Material [20]). In the measurements, the contacts for current (I) and voltage (V) are swapped for positive and negative fields. Pressure in all measurements is determined by the ruby fluorescence method [21].

Figure 1 displays the temperature dependence of electrical resistance at different pressures. We find that the superconducting transition temperature (T_c) of sample 1 increases upon elevating pressure and then decreases upon further compression [Figs. 1(a) and 1(b)], in good agreement with the results reported previously [22–27]. Similar results were obtained in the measurements on sample 2 [Figs. 1(c) and 1(d)], i.e., T_c first shows an increase in the low pressure range, reaches a maximum value, and then decreases with further pressurizing. At about 12 GPa, the superconductivity is completely suppressed [Fig. 1(d)]. We repeated the measurements with new samples in five independent experiments and obtained reproducible results.

To know the connection between the superconductivity and the electronic state in $FeTe_{0.55}Se_{0.45}$, we performed high-pressure measurements on Hall resistance (R_{xy}) by sweeping the magnetic field (B), applied perpendicular to the *ab* plane, from 0 to 2 T on a single crystal sample at various temperatures, as shown in Figs. 2(a)–2(e). $R_{xy}(B)$ is negative below 33 K at 0.5 GPa, 28 K at 1.8 GPa, 23 K at 2.4 GPa, respectively. However, at the pressures above 3.4 GPa, the plots of the $R_{xy}(B)$ are positive within the temperature range investigated. These results indicate that an electron-hole carrier balance ($R_{xy}(B) = 0$) at the critical temperatures (T^*) occurs only below 3.4 GPa. Since the maximum T_c of the pressurized $FeTe_{0.55}Se_{0.45}$ is about 22 K, the fixed temperature of 23 K is chosen for the isothermal pressure measurements of the Hall coefficient so as to make a reasonable comparison on the Hall coefficients obtained from different pressures. In this case, the critical pressure where $R_{xy}(B) = 0$ is estimated to be ~2.7 GPa (as shown in Fig. 2(f) and the Supplemental Material [20]).

To visualize the correlation between T_c and electronic state in $FeTe_{0.55}Se_{0.45}$, we summarize our experimental results in Fig. 3, which demonstrates R_H, T_c and structure information of the $FeTe_{0.55}Se_{0.45}$ at different pressures. It is seen that T_c is significantly enhanced upon increasing pressure in the pressure range of $0 < P < P_c$ (~2.7 GPa), as shown in the lower panel of Fig. 3, while the R_H derived from the Hall resistance R_{xy} becomes less negative (see upper panel of Fig. 3 and the Supplemental Material [20]), reflecting that the contribution of hole carriers to the T_c enhancement is increased.

The connection between the electron state and the lattice structure is one of the key issues for understanding the emergence of the exotic phenomena in correlated electron materials [28,29]. Interestingly, we noted that the high resolution x-ray diffraction (XRD) measurements find a temperature-

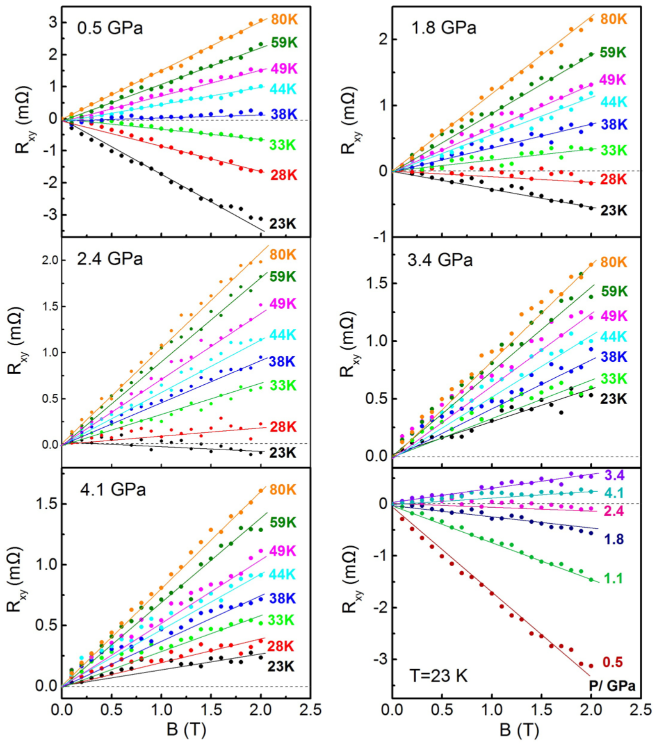

FIG. 2. Hall resistance (R_{xy}) as a function of magnetic field (B) for the $FeTe_{0.55}Se_{0.45}$ single crystals. Plots of R_{xy} versus B at different temperatures in the pressure range of (a) 0.5 GPa, (b) 1.8 GPa, (c) 2.4 GPa, (d) 3.4 GPa, and (e) 4.1 GPa. (f) R_{xy} versus B at 23 K for pressures ranging from 0.5 to 3.4 GPa. The solid lines are guides to the eye. The dashed line indicates $R_{xy}(B) = 0$ where the pressure is estimated to be ∼2.7 GPa.

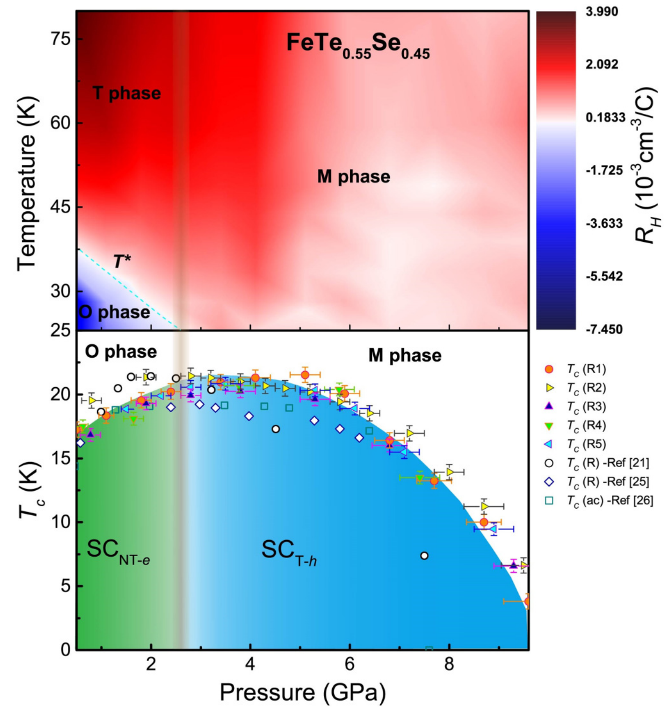

FIG. 3. Hall coefficient (R_H), structure, and superconducting transition temperature (T_c) information of the $FeTe_{0.55}Se_{0.45}$ superconductor at different pressures. Upper panel presents the mapping information of temperature and pressure dependent R_H, shown in color scale. Here T^* represents the temperature of the electron-hole carrier balance. T, O, and M stand for the tetragonal, orthorhombic, and monoclinic phases, respectively. Lower panel displays T_c as a function of pressure. The values of T_c are determined by the midpoint of the superconducting transition. SC_{NT-e} and SC_{T-h} represent the nontrivial superconducting phase with the dominance of electron carriers and the trivial superconducting phase with the dominance of hole-carriers, respectively. T_c(R1), T_c(R2), T_c(R3), T_c(R4), and T_c(R5) stand for the T_c obtained by the resistance measurements for sample 1, sample 2, sample 3, sample 4, and sample 5. T_c(ac) and T_c(R) represent the T_c obtained by the *ac* susceptibility and resistance measurements.

induced structural transition of the tetragonal-orthorhombic (T-O) phase at ∼40 K in the $FeTe_{0.43}Se_{0.57}$ superconductor [25]. Also, a pressure-induced transition from O phase to monoclinic (M) phase was observed in the same sample at ∼2.5 GPa below 40 K [25]. Because the composition of the superconductor used for the high pressure XRD measurements is nearly the same as that of our sample, and, in particular, its ambient-pressure transition temperature (∼40 K) of the T-O phase and the pressure-induced O-M phase transition at low temperature (at ∼2.5 GPa) are on the line of our $T*(P)$ (upper panel of Fig. 3), we propose that our samples should share the same structure phase transitions to that of the $FeTe_{0.43}Se_{0.57}$ superconductor upon cooling at ambient pressure or at the P_c (∼2.5 GPa) in the low temperature range. We find that T^* decreases with increasing pressure below P_c (blue region of the upper panel) until undetectable at $\sim P_c$ where the O-M phase transition takes place [25]. This implies that, from ambient pressure to P_c, the transport property of the normal state becomes more p type upon increasing pressure. Around the P_c, T_c of the orthorhombic superconducting phase reaches to a maximum. On further compression above P_c, T_c decreases, while $R_H(P)$ undergoes a sign change from negative to positive, as signified by the change of the color from blue to red (see upper panel of Fig. 3 and the Supplemental Material [20]).

The sign change of R_H in materials is usually associated with a reconstruction of the electronic structure on the Fermi surface (FS) [30–33], so that it can be taken as a fingerprint to manifest the FS reconstruction. Our results demonstrate a close correlation between the FS reconstruction and the T-O or the O-M phase transition. It is interesting to note that the ambient-pressure neutron scattering measurements on superconducting $Fe_{1.08}Te_{0.64}Se_{0.33}$ [34] and $FeTe_{0.5}Se_{0.5}$ [9], whose compositions are similar to that of our sample, show that there are no long-rang magnetic order exist in the samples, but the short-range magnetic correlations with the incommensurate excitation in the superconducting phases. Moreover, ARPES studies found that the normal state of the $FeTe_{0.58}Se_{0.42}$ superconductor presents a strongly correlated metallic feature, which hosts the effective carrier mass up to $16m_e$ [35]. Based on our results and analysis, we propose that the nontrivial superconductivity of this class of materials [11,12] may be associated with the interplay between FS reconstruction and the lattice change, which generates the unusual normal state

In addition, the observed O-M phase transition at the pressure above P_c leads us to propose that the sample may lose its nontrivial superconductivity due to the corresponding change of its crystal structure symmetry needed for protecting the nontrivially topological property [36–39]. Considering no significant change in $R_H(P)$ in the M phase (see the upper panel of Fig. 3 and the Supplemental Material [20]), we suggest that the pressure-induced instability, i.e., the extent of its lattice distortion, of the M phase is responsible for the T_c decrease.

In conclusion, an intimate correlation among the sign change of R_H (a fingerprint for the reconstruction of the Fermi surface), structural phase transition, and T_c in the putative topological superconductor $FeTe_{0.55}Se_{0.45}$ has been revealed by our high pressure studies. We find that a noticeable sign change in R_H influences its superconducting transition temperature remarkably. The nontrivially topological superconductivity can be stabilized up to 2.7 GPa (P_c), but it may no longer exists above P_c due to a crystal structural phase transition. Our results suggest that the nontrivial superconductivity in this material may be associated with its unusual normal state featured by the dramatic interplay between the electronic state and the lattice change. We hope that the correlation among the sign change of R_H, structural phase transition and T_c found in this study will shed new light on understanding the entangling state among superconductivity, electronic and lattice structure, and such an entangling state should be responsible for the presence of the nontrivially topological nature of this topological superconductor.

The work in China was supported by the National Key Research and Development Program of China (Grant No. 2017YFA0302900, 2016YFA0300300, and 2017YFA0303103) and the Strategic Priority Research Program (B) of the Chinese Academy of Sciences (Grant No. XDB25000000). J. G. is grateful for support from the Youth Innovation Promotion Association of the CAS (2019008). Work at Penn State was supported by the U.S. National Science Foundation under Grant No. DMR1707502.

[1] Y. Kamihara, T. Watanabe, M. Hirano, and H. Hosono, J. Am. Chem. Soc. **130**, 3296 (2008).

[2] B. Keimer, S. A. Kivelson, M. R. Norman, S. Uchida, and J. Zaanen, Nature (London) **518**, 179 (2015).

[3] F. C. Hsu, J. Y. Luo, K. W. Yeh, T. K. Chen, T. W. Huang, P. M.Wu, Y. C. Lee, Y. L. Huang, Y. Y. Chu, D. C. Yan, and M. K.Wu, Proc. Natl. Acad. Sci. USA **105**, 14262 (2008).

[4] S. Medvedev, T. M. McQueen, I. A. Troyan, T. Palasyuk, M. I.Eremets, R. J. Cava, S. Naghavi, F. Casper, V. Ksenofontov, G. Wortmann, and C. Felser, Nat. Mater. **8**, 630 (2009).

[5] J. P. Sun, K. Matsuura, G. Z. Ye, Y. Mizukami, M. Shimozawa, K. Matsubayashi, M. Yamashita, T. Watashige, S. Kasahara, Y. Matsuda, J.-Q. Yan, B. C. Sales, Y. Uwatoko, J.-G. Cheng, and T. Shibauchi, Nat. Commun. **7**, 12146 (2016).

[6] K. W. Yeh, T. W. Huang, Y. L. Huang, T. K. Chen, F. C. Hsu, P.M. Wu, Y. C. Lee, Y. Y. Chu, C. L. Chen, J. Y. Luo, D. C. Yan, and M. K. Wu, EPL **84**, 37002 (2008).

[7] Y. Qiu, W. Bao, Y. Zhao, C. Broholm, V. Stanev, Z. Tesanovic, Y. C. Gasparovic, S. Chang, J. Hu, B. Qian, M. Fang, and Z. Mao, Phys. Rev. Lett. **103**, 067008 (2009).

[8] T. J. Liu, J. Hu, B. Qian, D. Fobes, Z. Q. Mao, W. Bao, M. Reehuis, S. A. J. Kimber, K. Prokeš, S. Matas, D. N. Argyriou, A. Hiess, A. Rotaru, H. Pham, L. Spinu, Y. Qiu, V. Thampy, A. T. Savici, J. A. Rodriguez, and C. Broholm, Nat. Mater. **9**, 718 (2010).

[9] H. A. Mook, M. D. Lumsden, A. D. Christianson, S. E. Nagler, B. C. Sales, R. Jin, M. A. McGuire, A. S. Sefat, D. Mandrus, T. Egami, and C. dela Cruz, Phys. Rev. Lett. **104**, 187002 (2010).

[10] S. Li, C. de la Cruz, Q. Huang, Y. Chen, J. W. Lynn, J. Hu, Y.-L. Huang, F.-C. Hsu, K.-W. Yeh, M.-K. Wu, and P. Dai, Phys. Rev. B **79**, 054503 (2009).

[11] P. Zhang, K. Yaji, T. Hashimoto, Y. Ota, T. Kondo, K. Okazaki, Z. Wang, J. Wen, G. D. Gu, H. Ding, and S. Shin, Science **360**, 182 (2018).

[12] D. Wang, L. Kong, P. Fan, H. Chen, S. Zhu, W. Liu, L. Cao, Y. Sun, S. Du, J. Schneeloch, R. Zhong, G. Gu, L. Fu, H. Ding, and H.-J. Gao, Science **362**, 333 (2018).

[13] H. Takahashi, K. Igawa, K. Arii, Y. Kamihara, M. Hirano, and H. Hosono, Nature (London) **453**, 376 (2008).

[14] X.-J. Chen, V. V. Struzhkin, Y. Yu, A. F. Goncharov, C.-T. Lin, Ho-kwang Mao, and R. J. Hemley, Nature (London) **466**, 950 (2010).

[15] L. L. Sun, X. J. Chen, J. Guo, P. W. Gao, Q. Z. Huang, H. D. Wang, M. H. Fang, X. L. Chen, G. F. Chen, Q. Wu, C. Zhang, D. C. Gu, X. L. Dong, L. Wang, K. Yang, A. G. Li, X. Dai, H. K. Mao, and Z. X. Zhao, Nature (London) **483**, 67 (2012).

[16] A. Drozdov, P. Kong, V. Minkov, S. Besedin, M. Kuzovnikov, S. Mozaffari, L. Balicas, F. Balakirev, D. Graf, V. Prakapenka, E. Greenberg, D. Knyazev, M. Tkacz, and M. Eremets, Nature (London) **569**, 528 (2019).

[17] M. Somayazulu, M. Ahart, A. K. Mishra, Z. M. Geballe, M. Baldini, Y. Meng, V. V. Struzhkin, and R. J. Hemley, Phys. Rev. Lett. **122**, 027001 (2019).

[18] J. Guo, Y. Zhou, C. Huang, S. Cai, Y. Sheng, G. Gu, C. Yang, G. Lin, K. Yang, A. Li, Q. Wu, T. Xiang, and L. Sun, Nat. Phys. **16**, 295 (2020).

[19] T. J. Liu, X. Ke, B. Qian, J. Hu, D. Fobes, E. K. Vehstedt, H. Pham, J. H. Yang, M. H. Fang, L. Spinu, P. Schiffer, Y. Liu, and Z. Q. Mao, Phys. Rev. B **80**, 174509 (2009).

[20] See Supplemental Material at http://link.aps.org/supplemental/10.1103/PhysRevB.101.214525 for details on the ambient pressure resistance measurements and high pressure Hall coefficient measurements.

[21] H.-K. Mao, J. Xu, and P. Bell, J. Geophys. Res. **91**, 4673 (1986).

[22] K. Horigane, N. Takeshita, C.-H. Lee, H. Hiraka, and K. Yamada, J. Phys. Soc. Jpn. **78**, 063705 (2009).

[23] J. Pietosa, D. Gawryluk, R. Puzniak, A. Wisniewski, J. Fink-Finowicki, M. Kozlowski, and M. Berkowski, J. Phys.: Condens. Matter **24**, 265701 (2012).

[24] A. Panfilov, V. Pashchenko, G. Grechnev, V. Desnenko, A. Fedorchenko, A. Bludov, S. Gnatchenko, D. Chareev, E. Mitrofanova, and A. Vasiliev, Low Temp. Phys. **40**, 615 (2014).

[25] N. C. Gresty, Y. Takabayashi, A. Y. Ganin, M. T. McDonald, J. B. Claridge, D. Giap, Y. Mizuguchi, Y. Takano, T. Kagayama, Y. Ohishi, M. Takata, M. J. Rosseinsky, S. Margadonna, and K. Prassides, J. Am. Chem. Soc. **131**, 16944 (2009).

[26] G. Tsoi, A. Stemshorn, Yogesh K. Vohra, Phillip M. Wu, F. C. Hsu, Y. L. Huang, M. K. Wu, K. W. Yeh, and Samuel T. Weir, J. Phys.: Condens. Matter **21**, 232201 (2009).

[27] S. I. Shylin, V. Ksenofontov, P. G. Naumov, S. A. Medvedev, V. Tsurkan, J. Deisenhofer, A. Loidl, L. M. Schoop, T. Palasyuk, G. Wortmann, and C. Felser, Phys. Status Solidi B **254**, 1600161 (2017).

[28] R. Mankowsky, A. Subedi, M. Forst, S. O. Mariager, M. Chollet, H. T. Lemke, J. S. Robinson, J. M. Glownia, M. P. Minitti, A. Frano, M. Fechner, N. A. Spaldin, T. Loew, B. Keimer, A. Georges, and A. Cavalleri, Nature (London) **516**, 71 (2014).

[29] J. P. Sun, G. Z. Ye, P. Shahi, J.-Q. Yan, K. Matsuura, H. Kontani, G. M. Zhang, Q. Zhou, B. C. Sales, T. Shibauchi, Y. Uwatoko, D. J. Singh, and J.-G. Cheng, Phys. Rev. Lett. **118**, 147004 (2017).

[30] J. Hu, T. J. Liu, B. Qian, and Z. Q. Mao, Phys. Rev. B **88**, 094505 (2013).

[31] D. Kang, Y. Zhou, W. Yi, C. Yang, J. Guo, Y. Shi, S. Zhang, Z. Wang, C. Zhang, S. Jiang, A. Li, K. Yang, Q. Wu, G. Zhang, L. Sun, and Z. Zhao, Nat. Commun. **6**, 7804 (2015).

[32] Y. Sun, T. Yamada, S. Pyon, and T. Tamegai, Sci. Rep. **6**, 32290 (2016).

[33] C. S. Zhu, J. H. Cui, B. Lei, N. Z. Wang, C. Shang, F. B. Meng, L. K. Ma, X. G. Luo, T. Wu, Z. Sun, and X. H. Chen, Phys. Rev. B **95**, 174513 (2017).

[34] W. Bao, Y. Qiu, Q. Huang, M. A. Green, P. Zajdel, M. R. Fitzsimmons, M. Zhernenkov, S. Chang, M. Fang, B. Qian, E. K. Vehstedt, J. Yang, H. M. Pham, L. Spinu, and Z. Q. Mao, Phys. Rev. Lett. **102**, 247001 (2009).

[35] A. Tamai, A. Y. Ganin, E. Rozbicki, J. Bacsa, W. Meevasana, P. D. C. King, M. Caffio, R. Schaub, S. Margadonna, K. Prassides, M. J. Rosseinsky, and F. Baumberger, Phys. Rev. Lett. **104**, 097002 (2010).

[36] L. Fu and C. L. Kane, Phys. Rev. B **76**, 045302 (2007).

[37] Y. Xia, D. Qian, D. Hsieh, L. Wray, A. Pal, H. Lin, A. Bansil, D. Grauer, Y. S. Hor, R. J. Cava, and M. Z. Hasan, Nat. Phys. **5**, 398 (2009).

[38] H. J. Zhang, C. X. Liu, X. L. Qi, X. Dai, Z. Fang, and S. C. Zhang, Nat. Phys. **5**, 438 (2009).

[39] J. P. Heremans, R. J. Cava, and N. Samarth, Nat. Rev. Mater. **2**, 17049 (2017).